TWENTY-SECOND INTERNATIONAL CONFERENCE ON COMPOSITE MATERIALS
(ICCM22)

BIOINSPIRED ARCHITECTURES TOWARD IMPROVING DAMAGE RESISTANCE ON CFRP LAMINATES

L. Amorim[1], A. Santos[1], J. P. Nunes[1] and J. C. Viana[1]

[1] IPC/i3N, University of Minho, 4804-533 Guimarães, Portugal, luis.amorim@dep.uminho.pt, www.dep.uminho.pt

Keywords: CFRP, Advanced composites, Bioinspired composites, Low velocity impact, Damage

ABSTRACT

Carbon fibre reinforced polymers (CFRP) are widely used in advanced applications due to their high performance and low weight, however, under certain conditions, they tend to develop internal damages that may compromise the component performance in service. Low velocity impact (LVI) events are one of the most common and dangerous solicitations that CFRP laminates must face during their life time, under these conditions they tend to develop so-called barely visible impact damages (BVID) that may propagate in service. To improve damage tolerance to LVI events, three new bioinspired CFRP laminates were developed and their mechanical properties and impact behaviour were compared to a typical aeronautic standard laminate in this work. All these studied laminates, having approximately the same thickness of 4 mm, were produced by vacuum bag infusion and observed under scanning electron microscopes (SEM) for assessing their processing quality. Tensile, interlaminar shear strength (ILSS) and LVI tests were performed in order to evaluate their Young's modules, global delamination resistance and impact response. LVI tests were performed for all laminates at the four different impact energy levels of 13.5, 25, 40 and 80 J and damage shape and areas were subsequentially evaluated by ultrasonic C-scan. SEM observations and the good agreement between theoretical and experimental Young's modules results demonstrated a processing quality. ILSS results have shown that the bioinspired hybrid laminate (HYB) presented better global resistance to delamination when compared to the other laminates. LVI tests and C-scan inspection have also demonstrated that HL and HL_S laminates exhibited higher resistance to damage propagation and smaller damaged area, respectively.

1 INTRODUCTION

Carbon fibre reinforced plastic (CFRP) laminates are being extensively used in advanced markets, such as aeronautic, defence, aerospace, among others, especially due to their high stiffness and low weight [1][2]. However, due to their layer-by-layer structural nature, when exposed to shear, impact or dynamic loading conditions, they may develop interlaminar damages. One of the most worrisome solicitations that they commonly may face in service is low velocity impact (LVI) events, which usually occurred during maintenance operations (dropping of tolls, for example), bird strikes, hailstone impacts, accidental collision of handling equipment, hard landings, among others. These kind of events may sometimes cause damages not easily detected by visual inspection, so-called barely visible impact damages (BVID), which can be source of development of much more severe internal damages in laminates, such as, resin cracks or delamination between layers [3].

Over the past years, biological laminate structures with outstanding impact properties have been seen as potential inspiration to mitigate damages caused by collisions on structural composites. An example of these structure can be founded on lobsters and crabs exoskeletons that present an microscale helical fibrous laminate structure (bouligand) [4][5].

This work aims to reproduce some of those biological laminate structures and other inspired on them in CFRP composites and, assess and compare their mechanical and impact behaviour with the one of a conventional aeronautic laminate.

2 APPROACH

The mechanical and impact properties of a conventional aeronautic laminate (LS) were compared with those ones obtained on other three bioinspired produced laminates, namely: a helical (HL), a helical-symmetric (HL_S) and a hybrid (HYB) laminate.

In order to mimic a bouligand structure, the HL laminate was produced with a layer sequence, in which a constant angle of 13,3º was maintained between plies. However, since this HL laminate showed significant twisting after curing due to its antisymmetric architecture along the thickness, the second laminate HL_S was built using a helical-symmetric structure with exactly the same pitch angle (13,3º) between plies to overcome the problem.

Based on the idea of generating a smooth transition angle between plies in order to reduce the damage on laminates, the HYB laminates were processed by using three thinner plies orientated in a way that ensured a soft transition between the direction used in each layer of the conventional LS laminate $[0/45/90/-45/45/-45/0]_{2S}$.

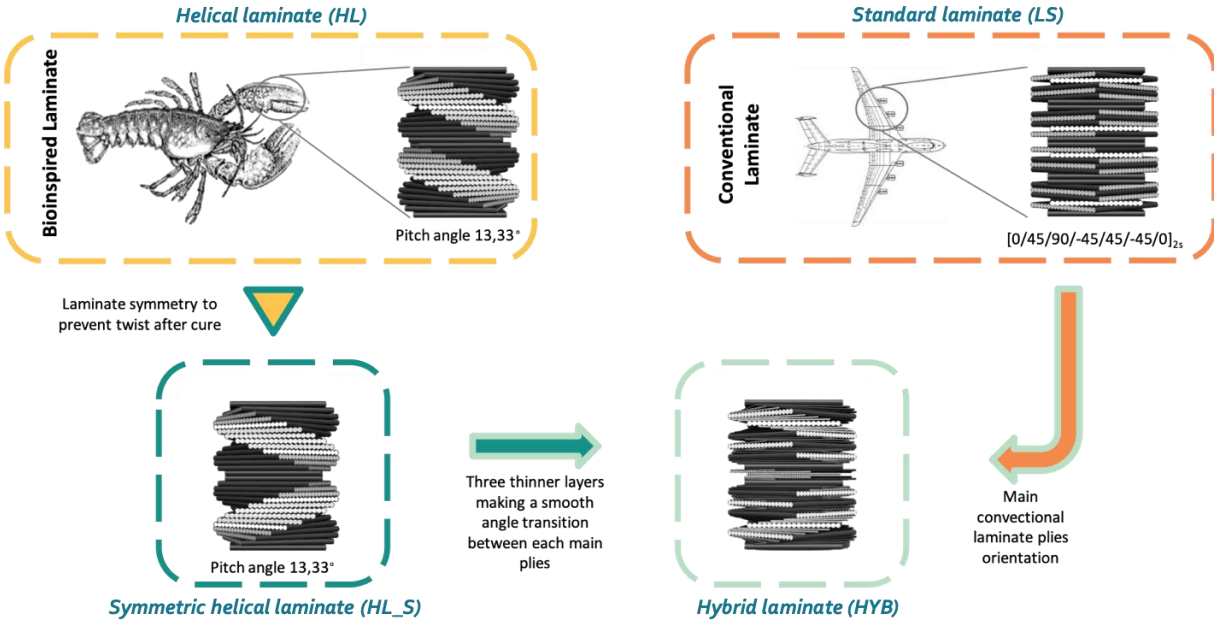

Figure 1: Approach schematic representation.

The LS, HL and HL_S laminates were produced using a 150 g/m^2 unidirectional carbon fibre fabric, which corresponds to a thickness of approx. 0.145 mm per final composite layer, whereas much thinner 50 g/m^2 unidirectional fabrics¸ corresponding to a thickness of approx. 0.05 mm per layer, were also used to interleave the main laminate layers in the HYB laminate. As matrix, it was used a bi-component epoxy resin (the Biresin® CR83 epoxy resin and Biresin® CH83-6 hardener, from Sika).

Table 1 summarises the stack sequence and number of UD carbon layers used in laminates.

Laminate Type	Nº of layers		Stacking Sequence
	150 g/m^2	*50 g/m^2	
LS	28	0	$[0/45/90/-45/45/-45/0]_{2S}$
HL	28	0	[0/13.3/26.6/…/360]
HL_S	28	0	$[0/13.3/26.6/\ldots/173.3]_S$
HYB	14	42	$[0/11.25^*/22.5^*/33.75^*/45/55.25^*/66.5^*/77.75^*/90/-77.75^*/-66.5^*/-55.25^*/-45/-22.5^*/0^*/22.5^*/45/22.5^*/0/-22.5^*/-45/-33.75^*/22.5^*/11.25^*/0/30^*/60^*/90^*]_S$

* layers using 50 g/m2 the interleave unidirectional carbon fibre fabric.

Table 1: Laminates stacking sequence.

3 EXPERIMENTAL TESTS

3.1 Laminates and processing characterization

After production, all laminates were observed by SEM in order to evaluate the adhesion quality between fibres and matrix (Figure 2 left) and the presence of voids (Figure 2 right).

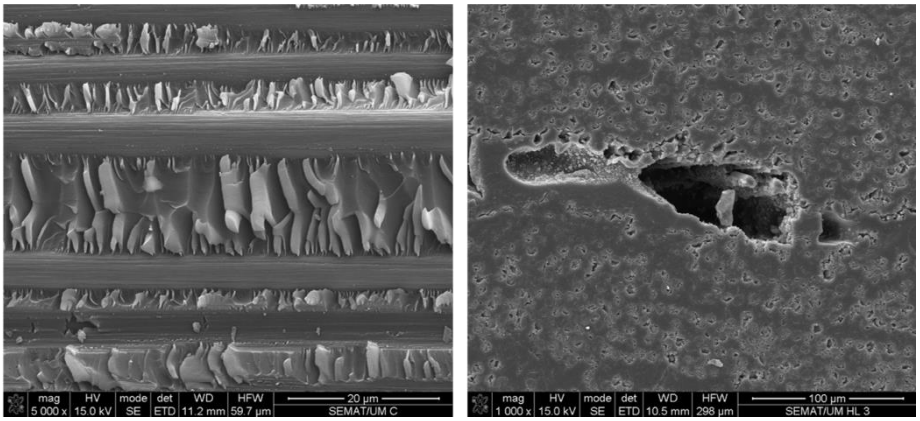

Figure 2: SEM visualisation of resin/fibres adhesion (5000 x) in LS laminate SEM (left) and void spot observe in HL laminate (1000 x) (right).

Before testing, the thicknesses were measured and the fibre volume fraction was determined by thermal gravimetric analysis (TGA) in all laminates. Table 2 presents the experimental results obtained.

Laminate Type	Thickness (mm)		Fibre volume fraction (%)
	Average	Std. Dev.	Average
LS	3.9	0.06	63.3
HL	3.8	0.08	65.1
HL_S	3.9	0.09	63.1
HYB	4.4	0.12	55.3

Table 2: Laminates properties.

3.1 Tensile tests

The theoretical Young's modules of each laminate were first theoretically determined by using the Classical Lamination Theory (CLT) and then compared with the results obtained by the tensile tests that were conducted using a universal testing machine according to the ASTM D3039/D3039M standard. Figure 3 presents the theoretical and experimental Young's modules obtained for each laminate.

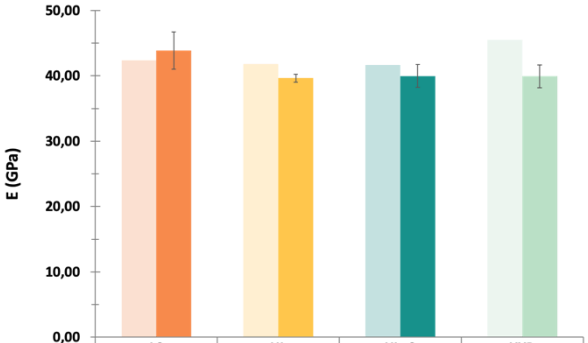

	LS	HL	HL_S	HYB
Theoretic	42,36	41,83	41,68	45,48
Experimental	43,86	39,65	39,96	39,94

Figure 3: Theoretical and experimental Young's modules results.

4.1 Interlaminar shear strength (ILLS) tests

ILSS tests were performed in accordance with ISO 14130 standard to evaluate and compare the influence of the different ply architectures used. Figure 4 shows the interlaminar shear strength results obtained from the ILSS tests.

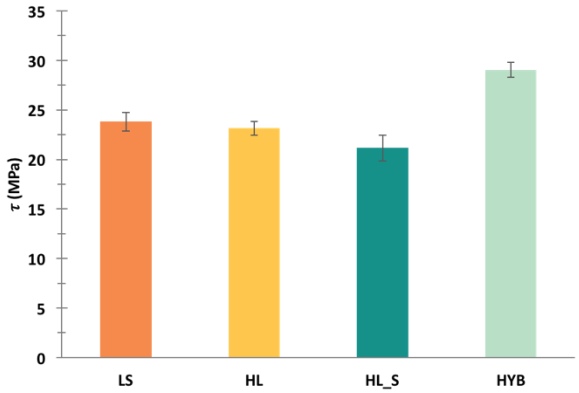

Figure 4: Interlaminar shear strength results.

4.1 Low velocity impact (LVI) tests

All laminates were submitted to LVI tests at four different impact energy levels (13.5, 25, 40 and 80 (J)) using a drop weight tower equipment following ASTM D7136/D7136M standard. Critical load (P_{cr}) and absorbed energy (E_{cr}) to onset damage propagation were determined by the simultaneous analysis of contact load and absorbed energy histories obtained in each tested sample. Figure 5 presents P_{cr} average results obtained from the LVI tests performed in the different laminates at 4 different energy impact levels.

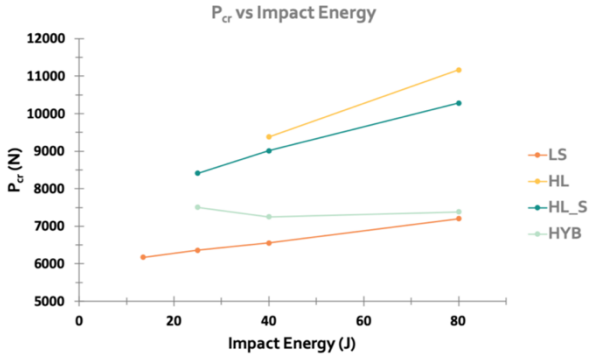

Figure 5: Average of critical load (P_{cr}) on different laminates as function of impact energy level.

After being impacted, all the specimens were scanned using an ultrasonic C-scan equipment in order to visualize the damage shape and afterword determine damaged area by the meaner of an acquisition and analyze image software.

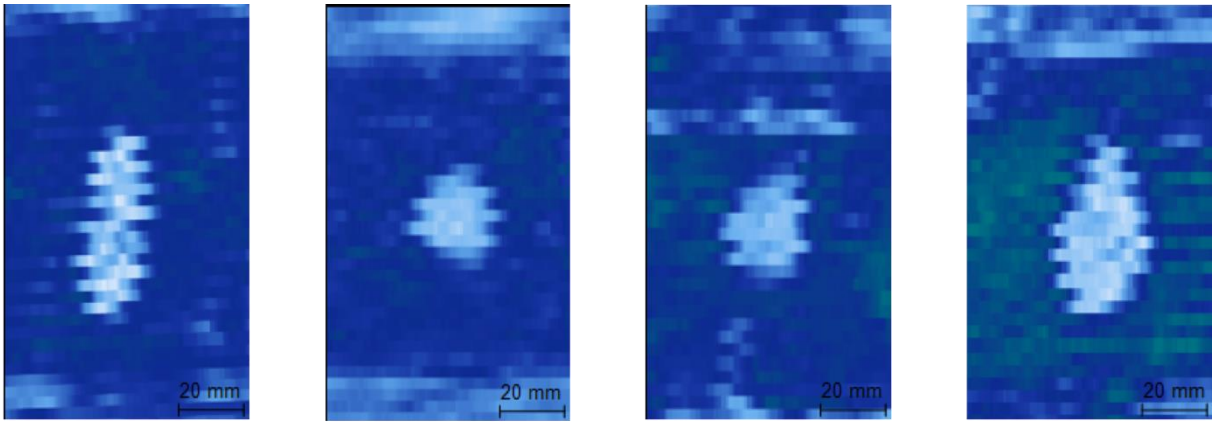

LS HL HL_S HYB

Figure 6: C-scan images of specimens impacted at 40 J.

Figure 6 shows a C-scan image of the laminates impacted at 40 J of impact energy and in Figure 7's chart are presented the damage area determined on each laminate for the different impact energy levels selected.

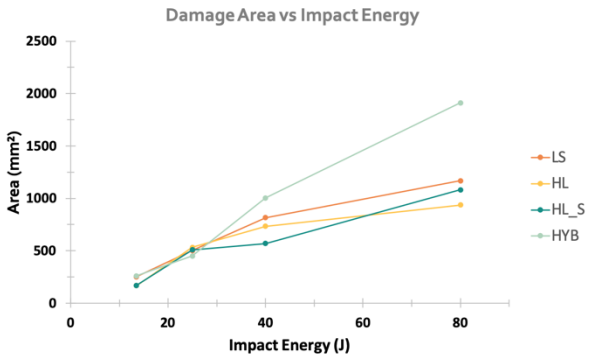

Figure 7: Damage area on laminates as function of impact energy level.

5 ANALYSIS AND DISCUTION

From the scanning electron microscopy (SEM) visualizations, was possible to observe a low void content and a good adhesion between carbon fibres and epoxy resin, confirming the good effectiveness and quality of the manufacturing process. The produced laminates presented almost the same thickness (~4 mm) and about 63% of fibre volume content, according the results obtained by thermal gravimetric analysis (TGA).

The tensile tests performed on the laminates have shown a good agreement between the experimental and the predicted theoretical results.

The results obtained from the ILSS tests showed that the bioinspired HYB laminate produced presented a global resistance to delamination 21.9 % higher than the standard one (LS). Under magnifier was also possible to observe that all bioinspired laminates presented mixed failure mode, showing simultaneously interlaminar shear and though-thickness fractures, while the LS one only by failed in interlaminar shear fracture mode.

Low velocity impact (LVI) tests made on all laminates at four different levels of impact levels have always demonstrated that, under these loading conditions, the three bioinspired laminates presented much better behaviour than the standard aeronautical laminate (LS). Regarding the critical load (P_{cr}) and energy (E_{cr}) to onset the damage, HL and HL_S laminates have shown to have a very similar behaviour in overall impact test conditions and much better results when compared to the other two laminates.

Finally, non-destructive ultrasonic inspections (C-scan) preformed on impacted specimen revealed that LS laminates tended to develop a typical composite peanut shape damage while HL and HL_S laminates presented a more localized concentric damage. HYB laminate has shown to be prone to develop lager and oval shape damages.

According to the measurements done on the analyze image software, up to 25 J of impact energy, all laminates presented roughly the same damaged area, however, for higher impact energy levels (40 and 80 (J)), HL and HL_S laminates have developed smaller damages than all the other laminates, while HYB laminates presented lager damaged area under these last impact conditions, very likely due to the higher number of interfaces inside the laminate.

9 CONCLUSIONS

In this work three new bioinspired laminates were compared to a standard aeronautic laminate, all produced by vacuum bag infusion, regarding their in-plan, interlaminar and low velocity impact performance. Process effectiveness was confirmed under scanning electron microscopy that have shown a low void amount inside the laminates and a good adhesion between fibres and epoxy resin. A good agreement was achieved between the theoretical and experimental Young's modules, confirming the good processing quality. The results obtained from ILSS tests showed an increase of 21.9 % in interlaminar shear strength by the HYB laminate, when compared to the others. LVI tests have demonstrated that all bioinspired laminates present higher tolerance to onset damage propagation when compared to the standard laminate (LS). Under C-scan inspections, HL and HL_S have shown to be prone to develop smaller and more localized damages when compared to the other laminates. Future work needs to be care out in order to identify and understand the mean damage mechanisms triggered by each laminate during the impact events.

ACKNOWLEDGEMENTS

The authors acknowledge the financial support of the project "IAMAT – Introduction of advanced materials technologies into new product development for the mobility industries" under the MIT-Portugal program exclusively financed by FCT- Fundação para a Ciência e Tecnologia. The authors also acknowledge PIEP (Centre for the Innovation in Polymer Engineering) for yielding of facilities and equipment.

REFERENCES

[1] R. M. JONES, *Mechanics of composite materials*, 2nd ed., no. 2. Taylor and Francis, Inc., 1999.

[2] Autar K. Kaw, *Mechanics of Composite Materials*, 2nd ed., vol. 29, no. Taylor & Francis, Inc., 2006.

[3] V. Tita, J. de Carvalho, and D. Vandepitte, "Failure analysis of low velocity impact on thin composite laminates: Experimental and numerical approaches," *Compos. Struct.*, vol. 83, no. 4, pp. 413–428, 2008.

[4] L. K. Grunenfelder *et al.*, "Bio-inspired impact-resistant composites," *Acta Biomater.*, vol. 10, no. 9, pp. 3997–4008, 2014.

[5] D. Ginzburg, F. Pinto, O. Iervolino, and M. Meo, "Damage tolerance of bio-inspired helicoidal composites under low velocity impact," *Compos. Struct.*, vol. 161, pp. 187–203, 2017.